

Symmetries of weighted networks: weight approximation method and its application to food webs

Julia Korol^{1,2} and Mateusz Iskrzynski*³

¹*Faculty of Mathematics, Informatics and Mechanics, University of Warsaw,
Warsaw, Poland*

²*Faculty of Mathematics, University of Vienna, Vienna, Austria*

³*Systems Research Institute, Polish Academy of Sciences, Warsaw, Poland*

June 16, 2025

Abstract

Knowing which parts of a complex system have identical roles simplifies computations and reveals patterns in its network structure. Group theory has been applied to study symmetries in unweighted networks. However, in real-world weighted networks, edge weights are rarely equal, making exact symmetry uncommon. To study symmetries in weighted networks, we aggregate edge weights into a small number of discrete categories. The symmetries of these aggregated networks identify vertices with similar roles in the original weighted network.

In food webs, this approach helps to quantify ecological co-existence and competition by assessing the functional substitutability of species. We apply our method to 250 empirical food webs, finding that symmetric vertices emerge even under weak approximations, typically forming small orbits of size two or three. These symmetric vertices can appear at any trophic level or network position. We also apply three symmetry measures to compare structural patterns at the network level.

*Correspondence: mateusz.iskrzynski@ibspan.waw.pl

1 Introduction

The study of network symmetries is one of the tools of complex network analysis, offering insights into the structural and functional properties of real-world systems. Traditional approaches to network symmetry, such as those based on graph automorphisms, focus on exact symmetries, where vertices can be permuted without altering the network's structure. These methods have two main limitations. First, they are not practical in weighted graphs, where even tiny numerical differences between edge weights can invalidate an exact symmetry. Second, they are highly sensitive to even minor changes in the network, such as the addition or removal of a single edge, and can be completely disrupted. This fragility makes exact symmetry measures less practical for real-world applications, where networks often exhibit near-symmetries or approximate symmetries due to the natural complexity of the system, noise, or model imperfections.

We address the first limitation and present a method to apply the network symmetry principle to weighted graphs. It considers copies of a network in which edge weights are iteratively approximated by their order of magnitude, then two orders of magnitude, and so on. Exact symmetries can then be studied in such approximated networks. We also study three network-level symmetry measures that capture different aspects of symmetry in graphs, and allow for comparison between graphs.

Our method could be said to study 'approximate symmetries', but several existing methods that disregard edge addition or removal have already applied this term. Examples demonstrating the idea and usefulness of approximate symmetries in this other sense range from 3D geometry [1] to differential equations [2]. [3] introduced the concept of approximate network symmetry. In that framework, a network is considered approximately symmetric if a permutation of its vertices preserves most, but not necessarily all, of its edges. That approach uses a simulated annealing algorithm to find the permutation that minimizes the number of edge mismatches, effectively quantifying how close the network is to being symmetric. However, this method has some drawbacks, including computational inefficiency and the assumption that permutations must not have fixed points — vertices that remain in their original position after permutation. Fixed points are important because they allow for partial symmetries, where only a subset of vertices is permuted, which is often the case in real-world networks.

Building on this, [4] proposed a more robust method called the Quadratic Symmetry Approximator. Unlike Liu's approach, it allows for fixed points, enabling the identification of partial symmetries and making it more suitable for analyzing real-world networks. [5] introduced a method to identify such approximate symmetries using a dynamical model, and called them quasi-symmetries. Still, even small weights, termed "weak links", were found to be significant for system

stability [6, 7], and their existence should not be neglected.

Symmetries in networks enable computational efficiency by reducing redundancy, which has driven much of their applications. When vertices in a network are symmetric, they share identical structural and functional roles, allowing computations performed on one vertex to generalize across its entire orbit. This reduces the need for repetitive calculations without losing critical information [8, 9]. In this way, symmetries can be exploited to optimize algorithms, reducing the computational burden in large networks [10], and allowing the aggregation of vertices with identical roles [11], thereby enabling a more efficient analysis of network properties.

Articles [10, 11] proposed that observed network symmetries can be explained by models in which vertices with similar degree tend to share similar linkage targets.

Beyond their technical and methodological utility, network symmetries can also reveal important properties of the underlying real-world systems. In food webs, for example, symmetries can help quantify the functional substitutability of species, offering new perspectives on coexistence and competition mechanisms. Thus, the study of network symmetries bridges methodological advancements with the exploration of real-world systems.

The coexistence of species is a fundamental concept in ecology, describing how different organisms can persist in the same ecosystem without outcompeting one another. The principle of competitive exclusion [12] posits that two species competing for the same limited resources cannot coexist indefinitely. However, in natural ecosystems, species often coexist despite overlapping resource requirements. This coexistence is facilitated by mechanisms such as resource partitioning, where species utilize different subsets of resources, and temporal or spatial segregation, where species avoid direct competition by occupying different *niches* in time or space [13, 14]. Additionally, the concept of the niche has been central to understanding coexistence, with [15] defining it as the multidimensional space of environmental conditions and resources that allow a species to survive and reproduce. Recent studies [16] have expanded this view, emphasizing the role of biotic interactions, such as predation and mutualism, in shaping coexistence dynamics. Symmetric vertices in food webs correspond to a 'trophic niche', which is defined by feeding relationships. This concept extends beyond resource constraints, which focus only on inflows to a vertex.

The degree of competition between species is often quantified through measures of niche overlap, which assess the similarity in resource use between two species. [17] introduced a widely used index to quantify niche overlap, calculated as the scalar product of the proportions of resources used by each species. This measure provides a quantitative basis for understanding how strongly two species compete for the same resources. However, competition is not always a binary

outcome; species may exhibit varying degrees of functional substitutability, where one species can partially or fully replace another in its ecological role. The degree of substitutability is influenced by factors such as the similarity in trophic levels, dietary preferences, and functional traits [18]. In food webs, the concept of substitutability can be extended through the lens of network symmetry, where species that occupy similar positions in the network (i.e., belong to the same automorphism orbit) can be considered functionally substitutable [8]. This approach allows for a more nuanced understanding of competition and coexistence in complex ecosystems.

One way to simplify ecological networks is through trophic species aggregation, where species with identical predators and prey are grouped together. This method, pioneered by [19] and [20], simplifies food web models by focusing on functionally equivalent groups rather than individual species. Similarly, in ecosystem modelling, species are often aggregated into functional groups based on shared traits such as diet, body size, or metabolic rates. They are then represented by one vertex (e.g., macrozooplankton). For example, [21] and [22] used functional group aggregation to study the stability and resilience of ecosystems. They demonstrated that clustering species with similar ecological roles can reveal general patterns in ecosystem organization. These methods align with the logic of network symmetries, as they both aim to reduce redundancy by focusing on the most critical components of the system.

In network science, spectral clustering and community detection algorithms offer another way to simplify complex networks by identifying groups of vertices (species or functional groups) that are densely connected or share similar structural roles. [23] and [24] developed and reviewed these methods, respectively, highlighting their utility in reducing the dimensionality of ecological networks. By grouping species into communities based on their connectivity patterns, these approaches provide a way to study coexistence mechanisms in a simplified yet meaningful framework. This is conceptually similar to the use of network symmetries, where symmetric vertices (species) are grouped into orbits, allowing for more efficient computation and analysis.

Finally, in metacommunity and metapopulation models, species or populations are often aggregated into meta-groups based on their spatial distribution, dispersal patterns, or habitat preferences. [25] and [26] applied these principles to study large-scale ecological systems, simplifying the analysis of species coexistence by focusing on groups of species or populations that behave similarly. These methods, like network symmetries, reduce complexity by identifying and leveraging functional or dynamical equivalence, enabling researchers to focus on the most critical interactions driving coexistence. Together, these approaches—trophic species aggregation, functional group modelling, spectral clustering, and metacommunity

theory—complement the study of species coexistence by providing technical tools to manage complexity and reveal the underlying structure of ecological networks.

In food webs, the vertices represent species or functional groups of species, and the edges represent the flow of biomass resulting from feeding relationships. The flows are averaged over, e.g., a period of a year. For a particular ecosystem the size of, e.g., a bay, there are two relevant large pools of accessible carbon: the atmosphere and dead organic matter. The atmosphere acts as an external pool of carbon dioxide, which is practically unlimited at the spatial scale of such an ecosystem and over time frames of years. Some organisms, such as phytoplankton, algae, and some bacteria, can assimilate carbon dioxide from the atmosphere. Thus, they are called primary producers and are biomass sources in the system. The second, spatially restricted pool of carbon is the dead organic matter, which is modelled as part of the food web. Dead organic matter suspended in the water, accumulated at the sea bottom, scattered over land, or contained in soil is referred to as detritus. All the other vertices are consumers, which feed on primary producers, detritus, or other consumers.

The symmetry of real-world networks provides information about structurally similar (or redundant) vertices. It can be considered as a local property of particular vertices, as in [27], as well as a feature of the graph as a whole. The global approach results in the introduction of symmetry measures. We choose three of them: redundancy [10, 28], symmetric vertices ratio [11], and the beta measure [29]. On the other hand, symmetry may also be described in terms of the spectral properties of a network [8], or its reduced versions [30], a direction that we do not follow in this study. [31], in turn, developed a method to compare symmetries of brain networks by graph matching.

Beyond the analysis of symmetry properties of food webs, we undertake a case study. We analyse the vertices that belong to one orbit under different edge weight aggregations in the Peruvian Upwelling ecosystem [32].

2 Methods and data

This section defines the key graph theoretical concepts, data, and tools used in our analysis. We introduce automorphisms, orbits, and the approximation of energy flows into weight classes, along with the symmetry measures applied. We introduce food webs and briefly outline the computational methods used.

2.1 Automorphisms and orbits

For a directed graph G with adjacency matrix ϕ , a graph *automorphism* σ is a permutation of the vertices $v \rightarrow \sigma(v)$ such that $\phi_{ij} = \phi_{\sigma(i)\sigma(j)}$ for all i, j . Analo-

gously, two vertices u, v are considered *symmetric* if there exists an automorphism $f : G \rightarrow G$ such that $v = f(u)$. For a more detailed explanation see e.g. [8].

Automorphisms split vertices into *orbits* containing vertices symmetric to each other. An orbit has only one element if no automorphisms map to it to any other vertex. An orbit containing more than one vertex will be called a *symmetric orbit* and its elements *symmetric vertices*.

2.2 Aggregating flows into classes

If edge weights in an empirical network accurately represented reality, typically no two weights would be equal. The only symmetric vertices would result from artificially repeated values, likely being the artifacts of modelling. To observe less trivial properties of the real system, we study approximate symmetries, by aggregating the flow values into discrete categories Φ_α , $\alpha \in \mathbb{N}$. The choice of Φ depends on the type of network in question and should be adapted to the weight distribution.

In a food web, the edge weights can span up to ten orders of magnitude [33]. We group together values differing by less than one or more orders of magnitude, defining a series of *aggregations* Φ_α ($\alpha = 0, 1, 2, 4, \dots$), approximating network flows

$$\Phi_\alpha(\phi_{ij}) = \begin{cases} \phi_{ij} & \text{for } \alpha = 0, \\ 1 + \lfloor \frac{\log_{10}(\phi_{max}) - \log_{10}(\phi_{ij})}{\alpha} \rfloor & \text{for } \alpha = 1, 2, 4, \dots \\ 1 & \text{for } \alpha = \infty. \end{cases} \quad (1)$$

where ϕ_{ij} is a flow between vertices v_i, v_j and ϕ_{max} is the flow with the highest value in the food web. Φ_0 is an identity function, and Φ_∞ assigns the same weight to each edge, converting a graph to its unweighted simplification. To ensure that flows grouped together by a previous aggregation belong to the same set in the following ones, we define α values as powers of two. In practice $\Phi_8 \sim \Phi_\infty$, as only few food webs contain flows that differ by more than eight orders of magnitude.

2.3 Symmetry measures

While the analysis of orbits and symmetric vertices reveals properties of individual vertices within a network, **graph symmetry measures** quantify the overall symmetry of the entire graph. This allows meaningful comparisons between different networks.

Let us consider a graph G with N vertices, N_O orbits, and N_S symmetric vertices.

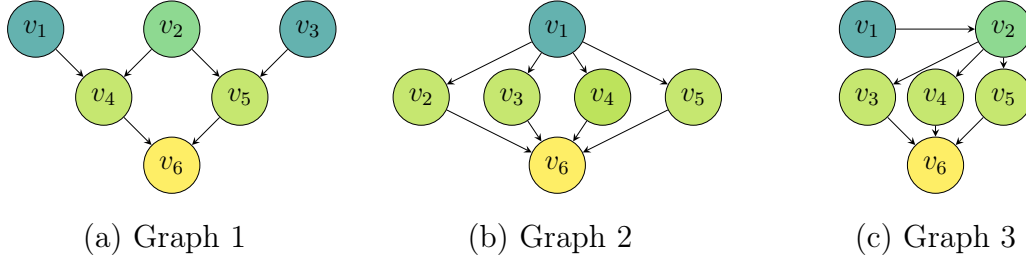


Figure 1: Three example graphs with the same number of vertices but with different structure of symmetry with orbits marked by colour. Graph (a) and (b) have the same number of symmetric vertices but different number of orbits. On the other hand, graphs (a) and (c) have the same number of orbits, but different number of symmetric vertices.

The symmetric vertices ratio, introduced in [11], is defined as:

$$S_V = \frac{N_S}{N} \quad (2)$$

This measure describes the proportion of vertices that are symmetric with respect to some nontrivial graph automorphism. Despite its intuitive appeal, graphs with differing symmetry structure can have the same value of S_V .

Consider the graphs shown in Fig. 1, each with $N = 6$. Graphs 1 and 2 have $S_{V,1} = S_{V,2} = \frac{4}{6} = 0.67$, while $S_{V,3} = \frac{3}{6} = 0.5$. Yet, S_V does not describe whether the symmetric vertices are connected through multiple independent automorphisms or just a few complex ones. **Redundancy**, proposed in [10], takes a complementary approach by focusing on the number of orbits:

$$r = \frac{N_O - 1}{N}, \quad r \in [0, 1) \quad (3)$$

This measure reaches its maximum when every vertex belongs to its own orbit (no symmetry), and is zero when all vertices are fully symmetric (i.e., belong to a single orbit).

Redundancy can yield different interpretations than S_V . For example, while Graph 3 has a lower S_V than Graph 1, they both have the same redundancy: $r_1 = r_3 = \frac{4-1}{6} = 0.5$. Graph 2 — previously tied with Graph 1 in S_V — has lower redundancy: $r_2 = \frac{3-1}{6} = 0.33$, suggesting it is more symmetric under this measure.

The Beta measure, proposed in [29], is defined as:

$$\beta = \left(\frac{|\text{Aut}(G)|}{N!} \right)^{1/N} \quad (4)$$

Here, $|\text{Aut}(G)|$ is the size of the graph's automorphism group, and $N!$ is the total number of possible permutations of N vertices. Thus, $\beta = 1$ corresponds to a fully symmetric graph, while $\beta = 0$ indicates a completely asymmetric one.

This measure is sensitive to the structure of the graph. In Graph 2, vertices v_1 and v_6 are asymmetric, but vertices v_2 through v_5 can be freely permuted, yielding $4!$ automorphisms. Hence,

$$\beta_2 = \left(\frac{1! \cdot 1! \cdot 4!}{6!} \right)^{1/6} \approx 0.567.$$

Similarly, Graph 3 has $3!$ automorphisms, resulting in $\beta_3 \approx 0.45$.

However, the symmetries in Graph 1 are more constrained. For example, if $v_1 \mapsto v_3$, symmetry requires $v_4 \mapsto v_5$. But if v_1 maps to itself, then v_4 must also map to itself. Since v_2 and v_6 are asymmetric, only two automorphisms are allowed: the identity and the one swapping (v_1, v_3) and (v_4, v_5) . Thus, $\beta_1 = \left(\frac{2}{6!} \right)^{1/6} \approx 0.375$.

2.4 Food webs

A food web represents an ecosystem as a set of species or functional groups of species (vertices) connected by flows of biomass resulting from feeding relationships. The most common models describe mass flows (measured in dry or wet weight), or closely related flows of carbon. Only a few models quantify the flow of nitrogen or phosphorus.

A food web is a weighted and directed graph of N vertices. An edge ϕ_{ij} represents the biomass flow from vertex j to vertex i . In this analysis we restrict ourselves only to local interactions between vertices representing living or non-living pools of biomass (detritus), ignoring exchanges with outside environment, such as atmosphere. These are usually also included in food web models as the import, export and respiration of each vertex.

2.5 Trophic level

In the 1940s, Raymond Lindeman introduced the concept of trophic levels to describe an organism's position in the food web. His model included five levels—from producers to top predators—and showed that biomass and energy flow decrease exponentially with each level, often by a factor of ten.

The cyclicity of biological processes described above makes the issue of assigning a trophic level to each vertex a non-trivial task. Traditionally, it was based on the shortest path from the source of biomass to a given organism. The modern approach [34] allows trophic levels to take non-integer values, capturing the complexity of real food webs through a recursive definition.

Trophic level 1 is assigned to non-living components and primary producers. For all other vertices, the trophic level is defined recursively as a biomass-weighted average of the levels of their resource vertices. If ϕ_{ji} denotes the biomass flow from vertex j to vertex i , then the trophic level τ_i is given by [34]

$$\tau_i := 1 + \sum_{j=1}^N \frac{\phi_{ij}}{\sum_{k=1}^N \phi_{ki}} \tau_j. \quad (5)$$

A unique solution exists under the condition that the food web is connected and 1 is not an eigenvalue of the diet proportion matrix $\left(\frac{\phi_{ij}}{\sum_{k=1}^N \phi_{ki}}\right)_{i,j} \in \mathbb{R}^{N \times N}$.

2.6 Dataset and automorphism computation

The analysed food webs, primarily describing marine ecosystems, originate from models published by ecosystem research groups. We provide their full bibliography in Supplementary Material. Most datasets were compiled from Ecopath with Ecosim [35] and retrieved from Ecobase [36].

To calculate food web automorphisms and their properties, we use the open source software SageMath [37].

3 Results

We apply the weight approximation method (Eq. 1) to explore symmetries in a dataset of 250 empirical food webs. While the raw data reveals almost no symmetries, many symmetric structures appear once flow values are approximated. We compare these results across different stages of aggregation to see how symmetry depends on the modelling approach.

Since each network vertex corresponds to a real species within an ecosystem, we focus on the characteristics of symmetric vertices and their orbits. We analyse the size and structure of these orbits and consider how they relate to ecological roles, particularly trophic levels. Finally, we compare three symmetry measures to evaluate how much distinct information they capture.

3.1 Case study: Peruvian Upwelling food web

An analysis of automorphism orbits in a specific ecological network can reveal structural patterns and functional roles. We demonstrate this using the Peruvian Upwelling food web [32] (see Fig. 2).

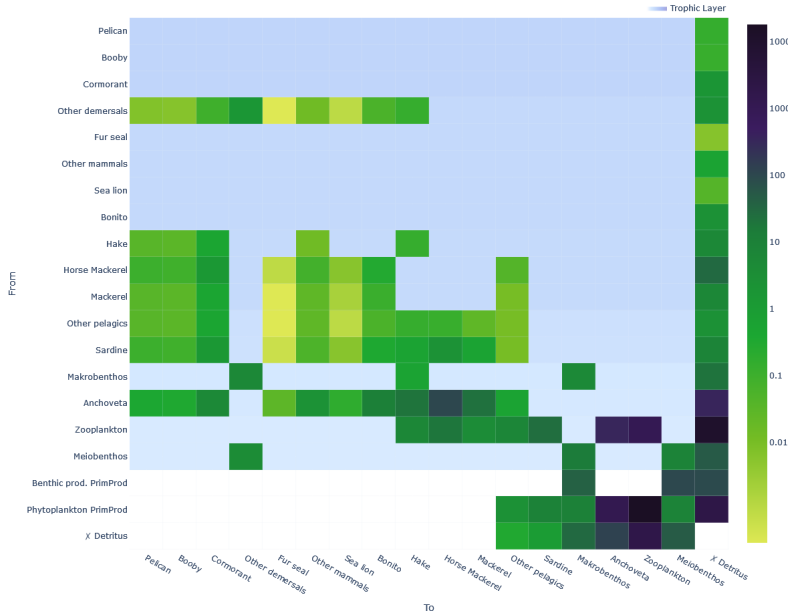


Figure 2: A heatmap representing the adjacency matrix of the Peru food web [32], drawn with foodwebviz [38]. The color of a cell maps the flow from the vertex in the row to the vertex in the column.

The Peruvian Upwelling food web consists of 20 vertices, making it relatively small compared to other food webs in the dataset. Without aggregation and under aggregation Φ_1 , this food web does not contain any symmetric orbits. Disregarding weight differences smaller than two and four orders of magnitude (in Φ_2 and Φ_4), two pairs of vertices are symmetric: $O_1^{\Phi_2} = \{\text{Booby}, \text{Pelican}\}$ and $O_2^{\Phi_2} = \{\text{Fur seal}, \text{Sea lion}\}$. Table 1 presents their mean trophic level and degree. The first orbit consists of two piscivorous bird species, while the second groups two species of pinnipeds. Disregarding weights in Φ_∞ completely merges the widened group of piscivorous birds with mammals, but also predatory bonito fish: $O_1^{\Phi_\infty} = \{\text{Fur seal}, \text{Sea lion}, \text{Booby}, \text{Pelican}, \text{Bonito}, \text{Cormorant}\}$. Another connects two mackerel species $O_2^{\Phi_\infty} = \{\text{Mackerel}, \text{Horse Mackerel}\}$. A third orbit $O_3^{\Phi_\infty} = \{\text{Sardine}, \text{Anchoveta}\}$ signals a functional similarity between two planktivorous fish, of which sardines are generally more omnivorous, while anchoveta sustain much higher biomass flows.

All symmetric vertices in this case have a total degree of seven or more. This is somewhat surprising, as one might expect that vertices with many connections would be harder to match and less likely to be part of a symmetric orbit. This underlines the highly nonrandom structure of food webs and the presence of important hidden variables, such as the physical size of considered organisms. Two

Orbit	Members	Φ_2			Φ_∞		
		Mean t.l.	$\deg(v)$	Members	Mean t.l.	$\deg(v)$	
O_1	{Fur seal, Sea lion}	3.35	7	{Fur seal, Sea lion, Booby, Pelican, Bonito, Cormorant}	3.34	7	
O_2	{Booby, Pelican}	3.32	7	{Mackerel, Horse Mackerel}	3.26	14	
O_3	-	-	-	{Sardine, Anchoveta}	2.47	15	

Table 1: Symmetric orbits present in Peru Upwelling food web under different aggregations. Columns *Mean t.l.* contain mean trophic level of vertices that are elements of orbits O_1, O_2, O_3 . We omit columns Φ_0 , Φ_1 as the Peruvian Upwelling food web is asymmetric under those aggregations, and Φ_4 as it contains exactly the same symmetries as Φ_2 .

species of similar size feed on species of sizes that are also similar. Physical and biological constraints limit the possibility of extending their interactions to completely different organisms. In this way, orbits summarise functional aspects of food webs that are shaped by such variables, even though these variables are not explicitly represented in the food web.

Table 2 presents the values of symmetry measures applied to the weight approximated copies of the Peru Upwelling food web. As we will see later in the text, the values of redundancy and the beta measure for the Peruvian Upwelling food web under aggregations Φ_2 and Φ_4 are typical for its size (see Fig. 5). However, under aggregation Φ_∞ , 50% of all vertices are considered symmetric. Peru's redundancy of 0.6 is among the lowest in the dataset.

	Φ_2			Φ_4			Φ_∞		
	r	S_V	β	r	S_V	β	r	S_V	β
Peru	0.85	0.2	0.13	0.85	0.2	0.13	0.6	0.5	0.18

Table 2: Values of symmetric measures symmetric vertices ratio S_V , redundancy r and the beta measure β of Peru Upwelling food web under different aggregations.

3.2 Properties of orbits

In this section, we analyse the set of all orbits in the consecutive aggregations of the 250 empirical food webs.

3.2.1 Size

Most of the orbits in our dataset contain two or three vertices. Even when considering higher aggregations, orbits rarely contain more than four vertices, as shown

in Fig. 3. The fact that only a few species groups in the ecosystem share the same functional role is aligned with the intuition developed by the competitive exclusion principle. This observation is also consistent with the fact that food web vertices often already represent aggregated functional groups.

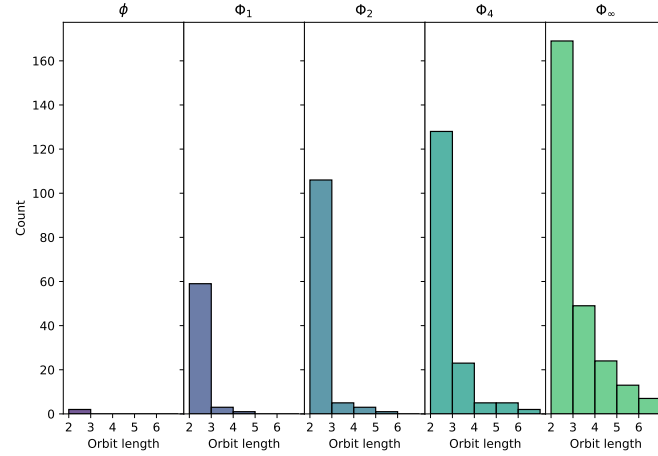


Figure 3: Histogram of symmetric orbit sizes with respect to different aggregations.

3.2.2 Trophic Properties

We analyse two aspects of the trophic structure in relation to symmetric orbits: the trophic span and the mean trophic level.

The trophic span of an orbit is defined as the difference between the maximum and minimum trophic level of the orbit's vertices. When no aggregation is used, vertices can only be symmetric if they have exactly the same trophic level. Fig. 4 (left) shows that in the approximations Φ_1, Φ_2, Φ_4 the trophic span remains below 0.5. In contrast, Φ_∞ which ignores edge weights, reveals that similarity in ecosystem functions can relate groups at more distant trophic levels.

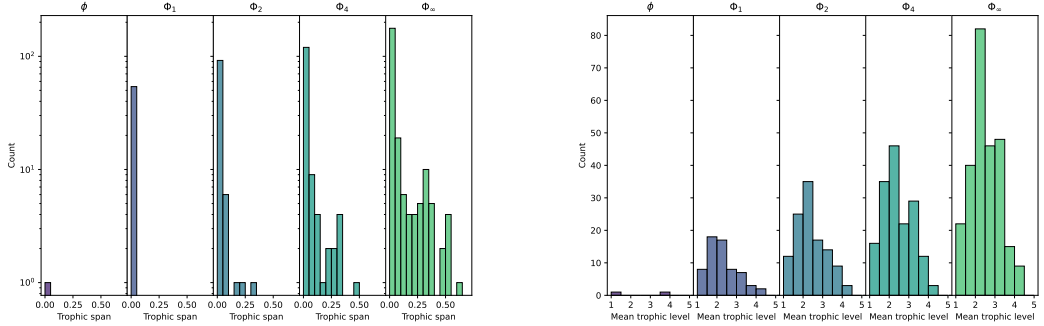


Figure 4: Symmetric orbits can be found at all trophic levels, but especially in the middle ones. The more we approximate edge weights, the larger is the possible difference in trophic levels between symmetric vertices. Left: the histogram of symmetric orbits trophic span, in logarithmic scale. Right: the histogram of symmetric orbits mean trophic level.

In terms of mean trophic level, symmetric vertices within the same orbit are typically found at trophic levels two or three (see Fig. 4, right). This range corresponds to the highly connected mid-trophic layers, where many interactions concentrate. Although one might expect high connectivity to imply structural asymmetry, we observe no such pattern.

3.3 Symmetry measures, network size and aggregation

Comparing the aggregations, we find that symmetry is common in transformed food webs, but almost absent in the originals. Only two untransformed networks contain any orbits, likely due to modeller choices. However, as shown in Table 3, aggregating weights up to one order of magnitude greatly increases symmetry, with similar symmetry measure distributions across all aggregations.

	ϕ	Φ_1	Φ_2	Φ_4	Φ_∞
Food webs with symmetries	2	36	57	71	96
Fraction	0.8%	14.4%	22.8%	28.4%	38.4%

Table 3: The number and fraction of food webs with nontrivial symmetries under each aggregation, relative to the full dataset.

Fig. 5 provides a quantitative overview of symmetry measures in our dataset. The most symmetric networks exhibit redundancy values above 0.8, indicating

that symmetric vertices group into small orbits. Typically, only a few symmetric vertices are present. However, when weights are ignored (in Φ_∞), some networks exhibit over 50% of vertices in non-trivial orbits. As evident in Fig. 5, all symmetry measures follow a highly skewed distribution.

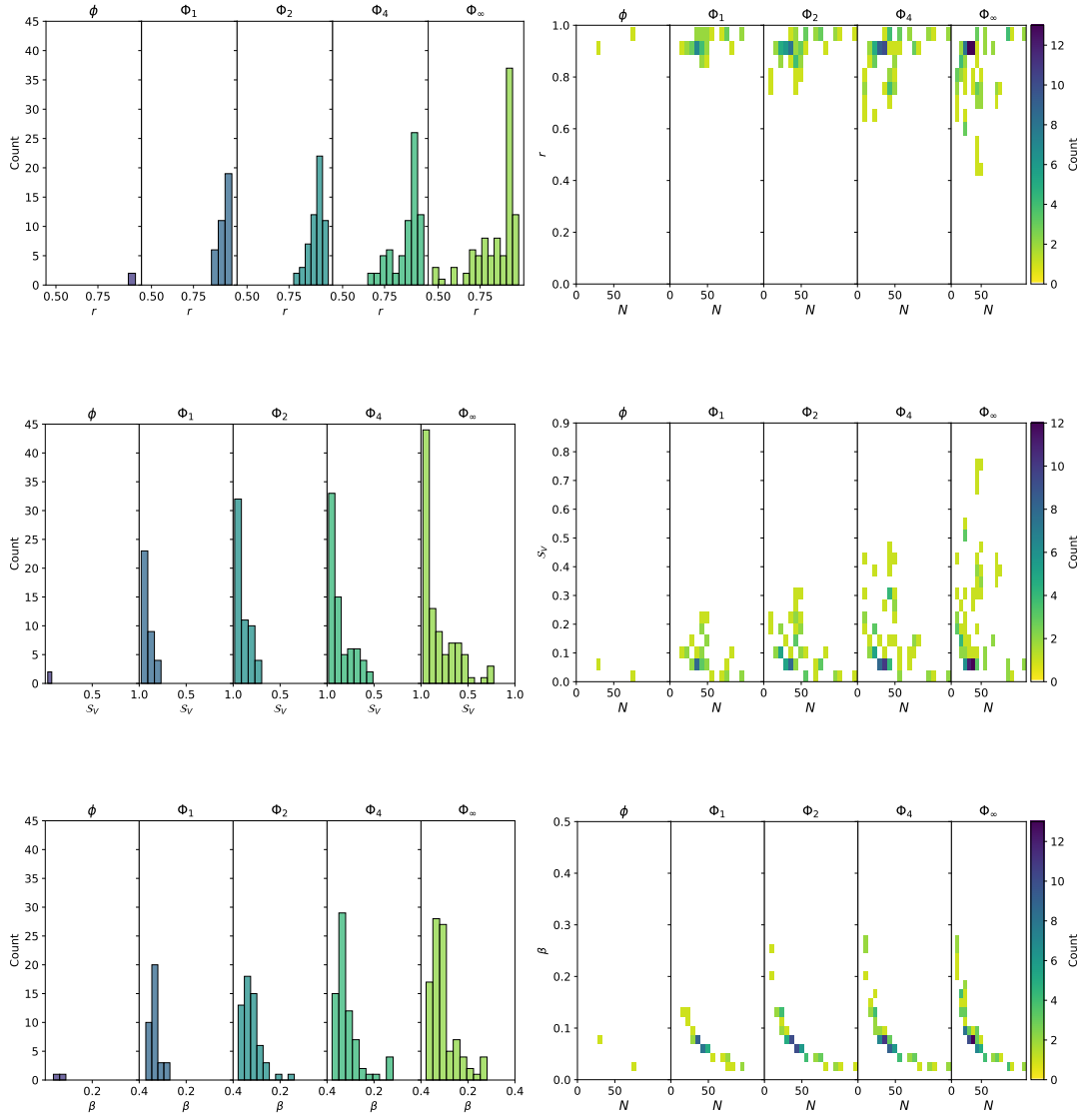


Figure 5: Left: histograms of symmetry measures. Colour maps the aggregation level. Right: two-dimensional histograms showing the relationship between symmetry measures and network size. The colour of each square represents the number of networks it contains. In all plots, fully asymmetric food webs are omitted.

The right panel of the Fig. 5 illustrates the relationship between symmetry measures and network size. Most symmetries (resulting in lower r , higher S_V , and β) appear in smaller graphs (fewer than 50 vertices), though even in the first aggregation, some networks with over 70 vertices exhibit symmetric orbits. As we have seen before, most networks have a redundancy value above 0.8. The exceptions, with lower redundancy, are mostly found in small networks, but some larger ones (around 75 vertices) can reach values as low as 0.7. Interestingly, smaller graphs show varying ratios of symmetric vertices, while even larger networks (over 50 vertices) can have more than 40% symmetric vertices.

The measure β follows the same curve for all graphs. In the food webs from the dataset, symmetries typically involve only a few vertices and orbits, leading to small automorphism groups. Consequently, the factorial term in its definition causes N to dominate the value of β . Thus, in the case of food webs, β values can be compared between networks of a similar size, but rarely between networks significantly differing in the number of vertices.

The summary of correlations between symmetry measures and the size of the networks is provided in the Table 4.

	Φ_1		Φ_2		Φ_4		Φ_∞	
	r_s	p_v	r_s	p_v	r_s	p_v	r_s	p_v
S_V vs N	-0.31	6.27×10^{-2}	-0.33	1.26×10^{-2}	-0.26	3.13×10^{-2}	-0.18	7.56×10^{-2}
r vs N	0.51	1.49×10^{-3}	0.51	5.14×10^{-5}	0.41	4.39×10^{-4}	0.26	9.53×10^{-3}
β vs N	-0.99	1.49×10^{-32}	-0.99	5.43×10^{-47}	-0.98	1.10×10^{-53}	-0.95	1.93×10^{-48}

Table 4: The correlation between symmetry measures quantified by the Spearman rank-order correlation coefficient. N is the number of vertices in the graph, r_s is the Spearman correlation coefficient, and p_v is the p-value of the test.

Table 4 shows that, for each measure, the correlation coefficients tend to approach zero as aggregation increases. Notably, the correlation between the symmetric vertices ratio and the number of vertices is weak. This suggests that the presence of symmetric vertices cannot be explained solely by the size of a food web.

Redundancy, across all aggregations, is more strongly correlated with N than the symmetric vertices ratio, though the relationship remains weak. For Φ_1 and Φ_2 , the Spearman coefficient (r_s) is close to 0.5 but decreases with increasing weight aggregation, reaching 0.26 for Φ_∞ . This may be a result of the structure of symmetry in the dataset. As shown in Fig. 3, most symmetric orbits contain only two vertices, regardless of the aggregation level. This type of symmetry affects the partitioning of orbits by changing their number by only one for each pair of symmetric vertices. The number of orbits with more than two vertices increases significantly for Φ_∞ , leading to an r_s value closer to 0.

The last measure, β , is almost fully correlated with network size (N). The value of r_s remains below -0.98 for all aggregations except Φ_∞ , where it reaches nearly -0.94. This indicates that, although symmetric vertices are present in the analysed food webs, they do not substantially increase the number of automorphisms in the corresponding automorphism groups.

3.4 Relations between symmetry measures

We examine the interdependencies between the vertex, orbit and automorphism aspects of symmetry. Fig. 6 presents the values of symmetry measure pairs for individual graphs. Table 5 summarises these relationships using Spearman correlation coefficients.

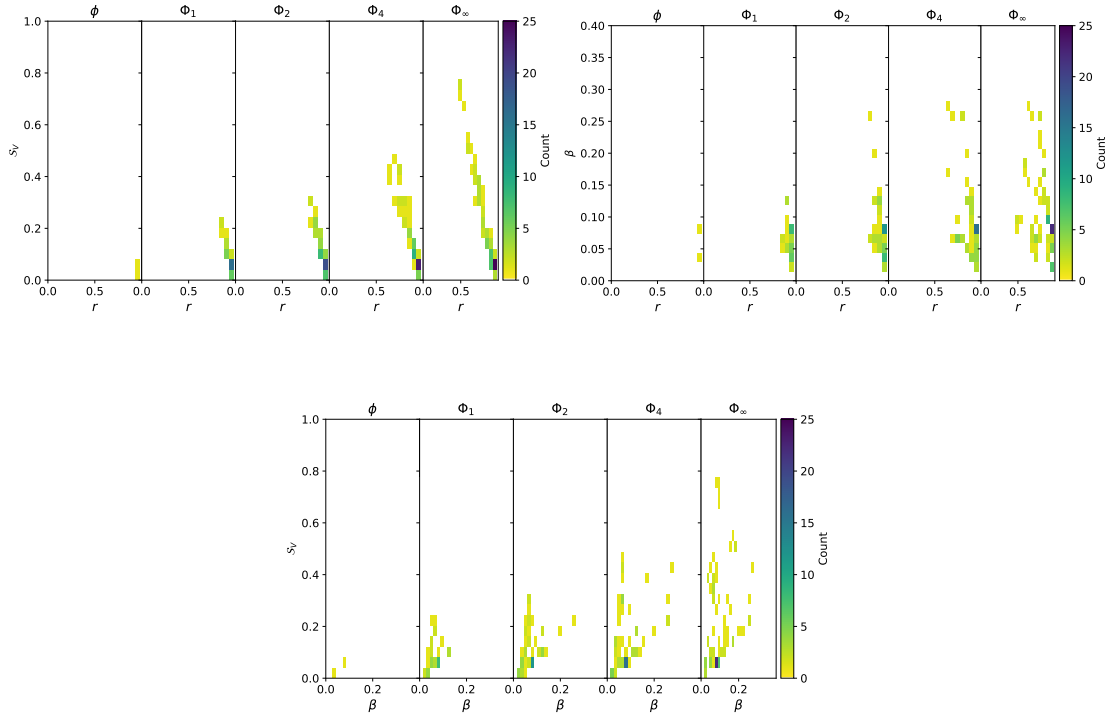


Figure 6: Two-dimensional histograms showing relations between symmetry measures. The colour of each square represents the number of networks within.

A strong relationship is observed between S_V and r , which reflects the dominance of small orbits, particularly those of length two. Since most vertices are asymmetric and form orbits of size one, the total number of orbits is high. Merging a few vertices into small symmetric orbits reduces this number only slightly, which

explains why redundancy remains above 0.5 even when up to 80% of vertices belong to symmetric orbits. The Spearman coefficient between these two measures, shown in Table 5, remains below -0.94 across all levels of aggregation, supporting this observation.

	Φ_1		Φ_2		Φ_4		Φ_∞	
	r_s	p_ν	r_s	p_ν	r_s	p_ν	r_s	p_ν
β vs r	-0.56	4.05×10^{-4}	-0.58	2.74×10^{-6}	-0.50	1.06×10^{-5}	-0.46	2.63×10^{-6}
β vs S_V	0.36	3.09×10^{-2}	0.40	2.28×10^{-3}	0.34	3.22×10^{-3}	0.38	1.68×10^{-4}
S_V vs r	-0.95	2.28×10^{-18}	-0.96	8.47×10^{-33}	-0.97	8.51×10^{-45}	-0.99	6.20×10^{-74}

Table 5: Correlation between symmetry measures based on the Spearman rank-order correlation coefficient. Notation follows Table 4.

The Spearman coefficient between β and r remains close to -0.5 across all aggregations, indicating a weak negative correlation. However, this correlation is stronger than that between β and S_V . This difference may be due to β and r both having a stronger correlation with the number of vertices in the graph.

4 Discussion

Approximate symmetry methods [1–5] identify structural similarities while allowing some edge mismatches, offering a complementary approach to our work. In food webs, small biomass flows contribute to ecosystem stability [6, 7], making edge removal-based approaches less suitable. However, combining weight approximation with selective edge exclusion could enable quantitative analyses of network symmetry.

Our dataset consists primarily of marine food webs, so the results may apply more directly to aquatic than terrestrial systems. Most terrestrial food web data lack complete quantitative measurements.

We define functional similarity as the minimum weight approximation needed for two species to share an orbit in the automorphism group. Such a measure could serve to quantify a trophic niche based purely on network structure.

Network models inherently simplify real systems through assumptions about edge presence and weight assignment. Some observed symmetries may reflect modelling choices rather than biological reality.

5 Conclusions

We have presented a method to identify vertices that have similar roles in a weighted network. We have extended automorphism-based approaches known for unweighted networks by aggregating edge weights into a few discrete categories. In this article, we have considered aggregations based on decimal orders of magnitude that work well for food webs.

The case study of the Peruvian Upwelling food web has revealed groups of species playing similar roles in this ecosystem that were all relatively well connected. We have also found that orbits, even though computed purely from graph structure, summarise functional aspects of food webs that are due to biological variables not present in the food web.

We have selected three network-level symmetry measures that capture independent symmetry properties - symmetric vertices, orbits, the size of the automorphism (symmetry) group. We have evaluated them using the proposed approximating procedure over a dataset of 250 empirical weighted food webs.

Symmetry orbits in food webs are small, often of size two. This leads to redundancy values above 0.8, and a strong relationship between the number of symmetric vertices and redundancy. Also, symmetric vertices in such small orbits do not substantially increase the number of automorphisms in the corresponding automorphism groups. Ecologically, the fact that only a few species share the same functionality aligns with the intuition developed by the competitive exclusion principle.

Symmetric vertices are found at various trophic levels. The ultimate aggregation, which ignores edge weights, reveals that similarity in ecosystem functions can relate groups at more distant trophic levels.

6 Acknowledgements

We thank Aleksandra Puchalska for her supervision of the mathematical side of the Bachelor thesis of Julia Korol, on which this article is based, and for the scrutiny around trophic level definition. We thank Ursula Scharler, Karol Opara, Elena Rovenskaya, Ulf Dieckmann, and Åke Brännström for their insights and discussions that aided Mateusz Iskrzyński in assembling the dataset of empirical food webs, due to be jointly published in connection with another study.

References

- [1] N. J. Mitra, L. J. Guibas, L. J. Guibas, M. Pauly, M. Pauly, Partial and approximate symmetry detection for 3d geometry, *ACM Transactions on Graph-*

ics (2006). doi:10.1145/1141911.1141924.

[2] M. Pakdemirli, M. Yürüşoy, İhsan Timuçin Dolapçı, Comparison of approximate symmetry methods for differential equations, *Acta Applicandae Mathematicae* (2004). doi:10.1023/b:acap.0000018792.87732.25.

[3] Y. Liu, Approximate network symmetry, arXiv: Physics and Society (2020). doi:10.48550/arXiv.2012.05129.

[4] A. Pidnebesna, D. Hartman, A. Pokorná, M. Straka, J. Hlinka, Computing approximate global symmetry of complex networks with application to brain lateral symmetry, *Information Systems Frontiers* (2025). doi:10.1007/s10796-025-10585-3.

[5] G. Rosell-Tarragó, A. Díaz-Guilera, Quasi-symmetries in complex networks: a dynamical model approach, *Journal of Complex Networks* (2021). doi:10.1093/comnet/cnab025.

[6] K. McCann, A. Hastings, G. R. Huxel, Weak trophic interactions and the balance of nature, *Nature* 395 (6704) (1998) 794–798. doi:10.1038/27427.

[7] C. Jacquet, C. Moritz, L. Morissette, P. Legagneux, F. Massol, P. Archambault, D. Gravel, No complexity–stability relationship in empirical ecosystems, *Nature Communications* 7 (2016) 12573. doi:10.1038/ncomms12573.

[8] R. J. Sánchez-García, Exploiting symmetry in network analysis, *Communications Physics* 3 (1) (May 2020). doi:10.1038/s42005-020-0345-z.

[9] P. Holme, Detecting degree symmetries in networks, *Phys. Rev. E* 74 (2006) 036107. doi:10.1103/PhysRevE.74.036107.

[10] B. D. MacArthur, R. J. Sánchez-García, J. W. Anderson, Symmetry in complex networks, *Discrete Applied Mathematics* 156 (18) (2008) 3525–3531. doi:10.1016/j.dam.2008.04.008.

[11] Y.-H. Xiao, W.-T. Wu, H. Wang, M. Xiong, W. Wang, Symmetry-based structure entropy of complex networks, *Physica A: Statistical Mechanics and its Applications* 387 (11) (2008) 2611–2619. doi:10.1016/j.physa.2008.01.027.

[12] G. F. Gause, *The struggle for existence*, Williams & Wilkins, Baltimore, 1934.

[13] P. Chesson, Mechanisms of maintenance of species diversity, *Annual Review of Ecology, Evolution, and Systematics* (2000). doi:10.1146/annurev.ecolsys.31.1.343.

- [14] P. Chesson, Updates on mechanisms of maintenance of species diversity, *Journal of Ecology* (2018). doi:10.1111/1365-2745.13035.
- [15] C. Hutchinson, Concluding remarks, *coldspring harbor symposium., Quant. Biol.* 22 (1957) 415–427.
- [16] J. M. Levine, J. Bascompte, J. Bascompte, F. R. Adler, P. B. Adler, S. Allesina, Beyond pairwise mechanisms of species coexistence in complex communities, *Nature* (2017). doi:10.1038/nature22898.
- [17] E. R. Pianka, Niche overlap and diffuse competition, *Proceedings of the National Academy of Sciences* 71 (5) (1974) 2141–2145. doi:10.1073/pnas.71.5.2141.
- [18] R. H. MacArthur, R. A. Levins, The limiting similarity, convergence, and divergence of coexisting species, *The American Naturalist* 101 (1967) 377 – 385.
- [19] P. Yodzis, K. O. Winemiller, In search of operational trophospecies in a tropical aquatic food web, *Oikos* 87 (2) (1999) 327–340. doi:10.2307/3546747.
- [20] R. J. Williams, N. D. Martinez, Simple rules yield complex food webs, *Nature* 404 (6774) (2000) 180–183. doi:10.1038/35004572.
- [21] E. A. Fulton, A. D. M. Smith, C. R. Johnson, Effect of complexity on marine ecosystem models, *Marine Ecology Progress Series* 253 (2003) 1–16. doi:10.3354/meps253001.
- [22] U. Brose, R. J. Williams, N. D. Martinez, Allometric scaling enhances stability in complex food webs, *Ecology Letters* 9 (11) (2006) 1228–1236. doi:10.1111/j.1461-0248.2006.00978.x.
- [23] M. E. J. Newman, Modularity and community structure in networks, *Proceedings of the National Academy of Sciences* 103 (23) (2006) 8577–8582. doi:10.1073/pnas.0601602103.
- [24] S. Fortunato, Community detection in graphs, *Physics Reports* 486 (3–5) (2010) 75–174. doi:10.1016/j.physrep.2009.11.002.
- [25] M. A. Leibold, M. Holyoak, N. Mouquet, P. Amarasekare, J. M. Chase, M. F. Hoopes, R. D. Holt, J. B. Shurin, R. Law, D. Tilman, M. Loreau, A. Gonzalez, The metacommunity concept: a framework for multi-scale community ecology, *Ecology Letters* 7 (7) (2004) 601–613. doi:10.1111/j.1461-0248.2004.00608.x.

- [26] I. Hanski, Metapopulation dynamics, *Nature* 396 (6706) (1998) 41–49. doi: 10.1038/23876.
- [27] P. Holme, Local symmetries in complex networks, *Journal of the Korean Physical Society* 50 (2007) 300–303. arXiv:cond-mat/0608695.
- [28] Y. Chen, Y. Zhao, X. Han, Characterization of symmetry of complex networks, *Symmetry* 11 (5) (2019). doi:10.3390/sym11050692.
- [29] B. D. MacArthur, J. W. Anderson, Symmetry and self-organization in complex systems (2006). doi:10.48550/arXiv.cond-mat/0609274.
- [30] D. Smith, B. Webb, Hidden symmetries in real and theoretical networks, *Physica A: Statistical Mechanics and its Applications* 514 (2019) 855–867. doi:10.1016/j.physa.2018.09.131.
- [31] C. Hu, G. Fakhri, Q. Li, Evaluating structural symmetry of weighted brain networks via graph matching, *Medical Image Computing and Computer-Assisted Intervention – MICCAI 2014* 17 (2014) 733–40. doi:10.1007/978-3-319-10470-6_101.
- [32] A. Jarre-Teichmann, D. Pauly, Seasonal changes in the peruvian upwelling ecosystem, in: V. Christensen, D. Pauly (Eds.), *Trophic models of aquatic ecosystems*. ICLARM Conference Proceedings, Vol. 26, 1993, pp. 307–314.
- [33] T. Okey, et al., A trophodynamic model of albatross bay, gulf of carpentaria: revealing a plausible fishing explanation for prawn catch declines, *CSIRO Marine and Atmospheric Research* (01 2006). doi:<https://doi.org/10.4225/08/5858239b3a821>.
- [34] D. Pauly, V. Christensen, J. Dalsgaard, R. Froese, F. Torres, Fishing down marine food webs, *Science* 279 (5352) (1998) 860–863. doi:10.1126/science.279.5352.860.
- [35] C. J. W. Villy Christensen, Ecopath with ecosim: methods, capabilities and limitations, *Ecological Modelling* 172 (2004) 109–139. doi:10.1016/j.ecolmodel.2003.09.003.
- [36] M. Colléter, A. E. Valls, J. Guitton, L. Morissette, F. F. Arreguín-Sánchez, V. Christensen, D. D. Gascuel, D. D. Pauly, Ecobase: A repository solution to gather and communicate information from ecosim models (2013). doi:<http://dx.doi.org/10.14288/1.0354309>.
- [37] W. Stein, et al., Sage Mathematics Software (Version x.y.z), The Sage Development Team, <http://www.sagemath.org> (YYYY).

[38] L. Pawluczuk, M. Iskrzyński, Food web visualisation: Heat map, interactive graph and animated flow network, *Methods in Ecology and Evolution* 14 (1) (2023) 57–64. doi:<https://doi.org/10.1111/2041-210X.13839>.